Vaporization Enthalpy and Cluster Species in Gas Phase of 1,1,3,3-Tetramethylguanidinium-Based Ionic Liquids from Computer Simulations

Guangren Yu, Xiaochun Chen and Charles Asumana
College of Chemical Engineering, Beijing University of Chemical Technology, 100029 Beijing, China

Suojiang Zhang and Xiaomin Liu
State Key Laboratory of Multiphase Complex Systems, Institute of Process Engineering, Chinese Academy of Sciences, 100190 Beijing, China

Guohui Zhou
Beijing Shengjinqiao Information Technology Co., Ltd., 100083 Beijing, China

DOI 10.1002/aic.12274
Published online May 20, 2010 in Wiley Online Library (wileyonlinelibrary.com).

In this work, the study on the volatility of ionic liquids is focused on the 1,1,3,3-tetramethylguanidinium-based ionic liquids. Vaporization enthalpy and cluster species in gas phase for 1,1,3,3-tetramethylguanidinium lactate ([tmgH][L]), 1,1,3,3-tetramethylguanidinium trifluoroacetate ([tmgH][T]), and 1,1,3,3-tetramethylguanidinium formate ([tmgH][F]), are investigated by using molecular dynamic simulation and ab initio calculation, respectively. Results from the molecular dynamic simulations show that the interionic interactions of coulombic electrostatic and Van der Waals forces are the main factors for deciding the volatility. In addition, owing to the change of molecular conformations from the liquid phase to the gas phase, intraionic bond, angle, and torsion interactions also give remarkable contributions. From the ab initio calculations, in the gas phase, an interionic proton transfer easily occurs in the ion pairs of these guanidinium-based ionic liquids, and the ion pairs are finally transformed into more thermodynamically stable neutral molecule dimers (this is different from some imidazolium-based ILs where ion pair can stably exist in gas phase). The transfer energy barriers are very low (typically, less than 2 kJ mol^{-1}). However, the existence of a third charged ion ($[tmgH]^+$, $[L]^-$, $[T]^-$, or $[F]^-$) or neutral molecule (tmg, HL, HT, or HF), will stabilize the ion pairs and prevent the transfer of proton. Finally, the stable trimers are then formed. The tetramers are also stable species. Ab initio results explain why they exist as ions in the liquid state. © 2010 American Institute of Chemical Engineers *AIChE J,* 57: 507–516, 2011

Keywords: ionic liquids, vaporization enthalpy, gas phase ion cluster, molecular dynamics simulation, ab initio calculation

Introduction

In the last few decades, ionic liquids (ILs), known as room-temperature ILs, have been receiving an upsurge of interest as neoteric solvents; mainly because of their unique chemical and physical properties, such as low-melting points

Additional Supporting Information may be found in the online version of this article.

Correspondence concerning this article should be addressed to X. Chen at chenxc@mail.buct.edu.cn.

(<100°C), nonvolatility (generally present undetectable vapor pressure), wide liquidus range, high thermal and chemical stability, nonflammability and recyclability.[1–5] ILs are often used in possible applications related to green chemical processes, viz liquid–liquid extractions, gas separations, catalysis, electrochemistry, fuel and solar cells, lubricants, functional materials, etc.[1–10]

Amongst the many desirable properties of ILs, we are particularly interested in their nonvolatility. Since ILs do not evaporate, they cannot lead to fugitive emissions; a feature that is doubtlessly important in engineering applications. As a matter of fact, nonvolatility is widely received as a defining characteristic of ILs,[11] and is one main reason why they are referred to as "green solvents."[4–7] For newly developed ILs, most people are likely to take their nonvolatility for granted. Almost all the applications of ILs in current studies are limited to the liquid phase, thus utilizing the advantage of nonvolatility.

Recently, although one distillation test showed that some ILs are volatile to some extent, and can be distilled at relatively lower pressure without decomposition; specifically some ILs of 1-alkyl-3-methylimidazolium bis(trifluoromethylsulfonyl)imide ($[C_nmim][Tf_2N]$).[11,12] On the one hand, while this unexpected result contradicts the widely held belief that ILs are nonvolatile, and on the other hand, it tends to pave the way for newer potential applications. For example, new purification methods, separation of two ILs by simple distillation as well as reactions that use ILs in the gas phase will become possible.[12] Earlier, the distillation and indirect determination of vapor pressure for some $[C_nmim][Tf_2N]$ ILs have been performed.[13–17]

A direct indicator for volatility is the value of vaporization enthalpy. The vaporization enthalpies for some imidazolium-based ILs have been calculated by using molecular dynamic simulations. The simulated values are in agreement with direct or indirect experimental measurement with acceptable errors.[17–25] The values of vaporization enthalpy are much higher than those of traditional molecule-style solvents (typically $>$ 100 kJ mol^{-1}; ~40 kJ mol^{-1} for H_2O at 373 K), indicating low volatility. Recently, the vaporization enthalpies of some $[C_nmim][Tf_2N]$ ILs were further systematically calculated in which volatile species with different sizes and compositions were assumed.[26] Ion pair was found to be the most possible volatile species with the lowest value of vaporization enthalpy, thereby supporting the assumption in all earlier simulations that volatile species is ion pair.

Ab initio calculations have been used to investigate the structure and interaction of ion pair or ion cluster in gas phase for ILs, especially for imidazolium-based ILs.[27–34] The results indicated that ion pair is stable in the gas phase. For more energetic triazolium-based ILs,[35] interionic proton transfer easily occurs in an ion pair to form neutral molecular dimer, and such a proton transfer was also found in the earlier study on ammonium dinitramide.[36] For some imidazolium-based ILs, the results from mass spectrometric analysis also indicated the existence of some ion cluster species in gas phase, such as $\{[mmim]_2[AlCl_4]\}^+$, $\{[mmim]_2[BF_4]_3\}^-$, $\{[mmim]_5[BF_4]_4\}^+$, and $\{[bmim]x\text{-}n[BF_4]x\}n^-$ (n=1, x=1~13; n=2, x=13~25).[37–40]

Guanidinium-based ILs have been used in gas absorption, organic synthesis, electrochemistry, analysis, etc.[41–47] The study on the volatility of guanidinium-based ILs is very valuable for expanding their applications and advancing the study on the volatility of ILs. However, up to now, this remains to be performed.

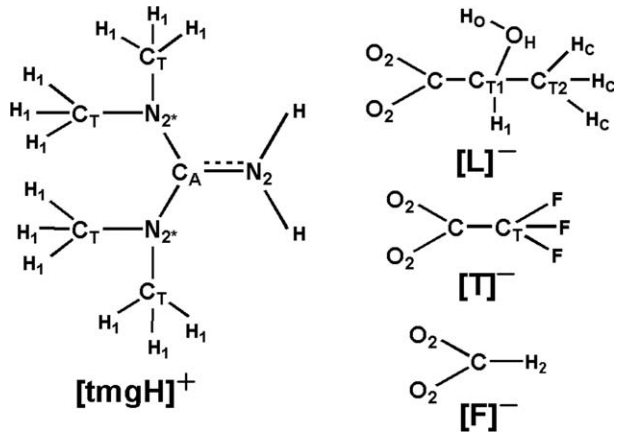

Figure 1. Structure of cation and anion for [tmgH][L], [tmgH][T], and [tmgH][F] (atoms are given in term of atom-type in AMBER force field from our previous work[51]).

Recently, we have performed a series of studies to understand the structure, interaction, and properties of some ILs in both the liquid and gas phases by using molecular dynamic simulation and ab initio calculation.[48–54] The force fields in the framework of AMBER for guanidinium-based ILs were developed,[51,54] the geometric and electronic structures of [tmgH][L] ion pair were investigated by using ab initio calculations.[49,50] In this work, the vaporization enthalpies of 1,1,3,3-tetramethylguanidinium lactate ([tmgH][L]), 1,1,3,3-tetramethylguanidinium trifluoroacetate ([tmgH][T]), and 1,1,3,3-tetramethylguanidinium formate ([tmgH][F]) are calculated by using molecular dynamic simulations (see Figure 1 for their molecular structures); their ion pair (cluster) species in gas phase are specified by using ab initio calculations. Following these results, a volatilization mechanism is discussed.

Computational Methods

Molecular dynamics simulation

The force field in the AMBER framework is from our previous work[51,54]; the simulation is performed with MDynaMix simulation package.[55] The simulation details for liquid phase are contained in our previous work[48,51,52,54]; the simulation system is composed of 256 ion pairs in *NPT* ensemble; the equilibrated and sampling time are 1 ns and 3 ns, respectively. Gas phase simulation is performed in *NVT* ensemble with one examined ion pair in simulation box, where the box diameter is 1000 Å. Longer equilibrated time (5 ns) and sampling time (10 ns) are adopted. Replicate runs are performed to estimate the uncertainty of simulation results. The configuration data in the production phase are used to perform the statistics on the distributions of bond, angle, and dihedral (the interval between two neighboring selected configurations is 100 time-steps).

Table 1. Vaporization Enthalpy (in kJ mol^{-1}) for [tmgH][L], [tmgH][T], and [tmgH][F], along with the Specific Contributions from Interionic and Intraionic Energies

		ΔU^{vap}									
		Interionic		Intraionic							
ILs	T (K)	LJ	Electrostatic	LJ	Electrostatic	Bond	Angle	Dihedral	Total	RT	ΔH^{vap}
[tmgH][L]	298	82.77	133.59	−2.33	−17.94	−33.11	−38.29	−19.59	105.10	2.48	108 ± 4
	318	83.25	137.62	−2.98	−18.37	−35.85	−40.71	−19.72	103.25	2.64	106 ± 4
	333	79.94	144.10	−2.95	−18.31	−37.44	−43.24	−20.22	101.88	2.77	105 ± 4
	373	78.94	148.91	−3.48	−19.02	−40.61	−46.05	−22.90	95.79	3.10	99 ± 4
[tmgH][F]	353	69.40	114.82	−1.46	−1.01	−30.93	−28.46	−19.64	102.71	2.93	106 ± 3
	373	67.66	120.73	−1.14	0.14	−32.34	−30.26	−23.87	100.91	3.10	104 ± 3
[tmgH][T]	318	73.14	119.15	−3.03	−7.31	−28.63	−29.94	−20.22	103.16	2.64	106 ± 4
	333	73.04	114.41	−3.06	−6.62	−30.96	−30.87	−20.26	95.68	2.77	98 ± 4

Ab initio calculation

Ab initio calculations are performed with GAUSSIAN 03 software package.[56] Density functional theory method B3LYP and frozen-core second-order perturbation approximation Møller–Plesset (MP2) are used to optimize geometry structure, combined with 6-31++G**basis set.[57–60] Zero point energy (ZPE) correction and frequency calculation are performed at the corresponding theory level, where the latter is used to specify the nature of each obtained structure, i.e., a true minimum or a transition state. Single point energy is improved at the higher level of MP2/6-311++g(2df,p).

Results and Discussion

Vaporization enthalpy

The vaporization enthalpy, ΔH^{vap}, is defined as[19,26]

$$\Delta H^{vap} = \Delta U^{vap} + RT \quad (1)$$

where R is gas constant, T is temperature, ΔH^{vap} is the change of internal energy between liquid phase and gas phase and is defined as

$$\Delta U^{vap} = U(vap) - U(liq) \quad (2)$$

The results of vaporization enthalpy for [tmgH][L], [tmgH][T], and [tmgH][F], are presented in Table 1. In Table 1, internal energy contributions are split into interionic and intraionic terms. Interionic contributions include Van der Waals (Lennard–Jones interaction potential, LJ) and coulombic electrostatic; whereas intraionic contributions include LJ, coulombic electrostatic, bond, angle, and dihedral.

From the data in Table 1, some conclusions can be drawn. First, interionic coulombic electrostatic interaction is the main contributor to vaporization enthalpy, with a ratio of about 40%, and interionic LJ interaction follows with a ratio of about 30%. The simulated vaporization enthalpy for some other ILs also showed that interionic interaction is the main contributor.[17–25] Second, the contributions from intraionic coulombic electrostatic and LJ interactions, however, are very small, especially the latter. Third, the intramolecular interactions from bond, angle and dihedral are remarkable, and the ratio is about 20%. Replicate run results show the certainties in vaporization enthalpy are around 3–4 kJ mol^{-1}, which is similar to that reported by Kelkar and Maginn.[26]

The remarkable contributions from bond, angle, and dihedral intramolecular interactions imply that the conformations in gas phase are somewhat different from that in liquid phase. The statistical results for bond, angle, and dihedral distributions for the three ILs are presented in Table 2. It can be indicated from Table 2 that (a) the distribution range of bond, angle, and dihedral is wider in liquid phase than in gas phase, i.e., the amplitude of molecular stretching or torsion is much larger in liquid phase, which can be attributed to much more interionic interactions in liquid phase; (b) compared with bond and angle distributions, dihedral distribution is wider in liquid phase, which means more free rotation of dihedrals.

The values of vaporization enthalpy for some imidazolium-based ILs at 298 K and 1 atm, are listed in Table 3. As shown in Table 3, the values of vaporization enthalpy for these ILs are almost at the same magnitude as those for some inorganic salts (e.g., silver chloride, 198 kJ mol^{-1}; cadmium fluoride, 214 kJ mol^{-1}),[62] while significantly higher for some traditional organic compounds (e.g., benzene, 30.7 kJ mol^{-1}, at 353 K and 1 atm), which is consistent with the nature of low volatility for ILs. The values of vaporization enthalpy for the currently investigated ILs are somewhat lower than those for the imidazolium-based ILs used in this study.

Ion species in gas phase

Dimer. The initial structures of gas phase ion pair for [tmgH][L], [tmgH][T], and [tmgH][F], are constructed through fully considering cation–anion interaction, such as interionic hydrogen bond, coulombic electrostatic, Van der Waals, and steric effect. The thorough scans of potential energy surface (PES) are performed to investigate the reaction path of interionic proton transfer in ion pair. The final structures of ion pair, transition state (TS), and molecular dimer, are obtained for [tmgH][L] (Figure 2), [tmgH][T] (Supporting Information Figure S1), and [tmgH][F] (Supporting Information Figure S2).

As for [tmgH][F], the stable structure of ion pair in gas phase is not found, only tmg·HF molecular dimer is obtained (Supporting Information Figure S2). A very similar reaction path and PES characteristic are found for [tmgH][L] and [tmgH][T]. Therefore, only the result of [tmgH][L] is used to discuss the dimer.

Table 2. Bond, Angle, and Dihedral Distributions in the Gas Phase and the Liquid Phase, for [tmgH][L] (at 298 K), [tmgH][T] (at 318 K), and [tmgH][F] (at 353 K)*

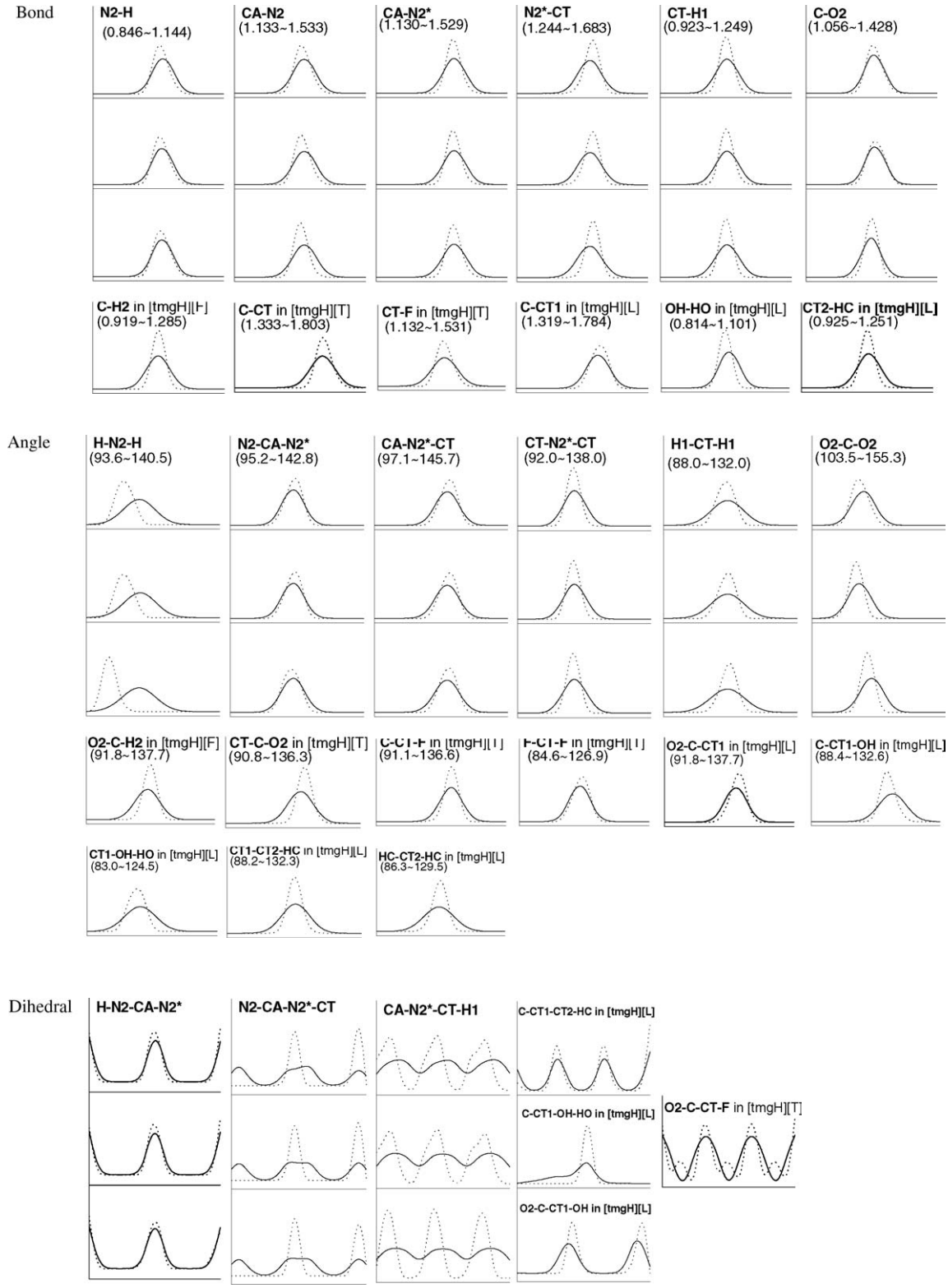

*Ordinate is probability, abscissa is statistical range (they are given in parentheses, and −180 to 180 for dihedral, length in Å and angle in degree). If not specifically stated, in one column the top is for [tmgH][L], the middle is for [tmgH][T], and the bottom is for [tmgH][F]. Dot line is in gas phase and solid line is in liquid phase.

Table 3. Vaporization Enthalpy (in kJ mol^{-1}) of ILs, at 298 K and 1 atm*

ILs	Vaporization Enthalpy	
	Simulation	Experiment
$[C_4mim][PF_6]$	172.0,[19]123.3,[22]** 161[20]	154.8,[15] 191.5[16]†
$[C_6mim][PF_6]$		139.8[15]
$[C_8mim][PF_6]$		144.3[15]
$[C_{10}mim][PF_6]$		135.9[15]
$[C_{12}mim][PF_6]$		112.0[15]
$[C_2mim][BF_4]$	161.3[19],255.8[22]**	
$[C_4mim][BF_4]$	161.8[19],252.9[22]**	128.2[15],203.5[16]†
$[C_8mim][BF_4]$		122.0[15]
$[C_{12}mim][BF_4]$		130.7[15]
$[C_2mim][NTf_2]$	159[17], 146[26]	135.3[14],136.1[15], 136[17]
$[C_3mim][NTf_2]$	172[17]	147[17]
$[C_4mim][NTf_2]$	174[17], 151[26]	134[16], 136.2[14],134.6[15], 193.5[16]†, 155[17]
$[C_5mim][NTf_2]$	179[17]	162[17]
$[C_6mim][NTf_2]$	184[17], 157[26]	139.8[14],141.6[15], 173[17]
$[C_7mim][NTf_2]$	186[17]	180[17]
$[C_8mim][NTf_2]$	201[17], 162[26]	149.0[14], 192[17]
$[C_{10}mim][NTf_2]$		155.5[15]
$[C_{14}mim][NTf_2]$		169.0[14]††
$[C_2mim][AlCl_4]$	225.2,[18]** 246.4[22]**	
$[C_4mim][AlCl_4]$	239.7[22]**	
$[C_4mmim][NTf_2]$		181.5[16]†
$[C_4mim][NO_3]$	130.2[22]**	
$[C_4mim][SbF_6]$		225.5[16]†
$[C_8mim][Cl]$		122.7[15]
$[C_4mim][CF_3SO_3]$		141.5[16]†
$[Ph(CH_2)mim][NTf_2]$		177.0[14,61]
$[Ph(CH_2)_2mim][NTf_2]$		188.0[14,61]
$[Ph(CH_2)_3mim][NTf_2]$		199.3[14,61]
$[Ph(CH_2)_3mim][PF_6]$		125.0[14,61]

*The superscript of the value is reference.
**The values are from *NVT* ensemble where *V* is defined in accordance with the experimental density.
†The values are obtained from the internal energies of vaporization in the literature, according to Eq. 1.
††At 308.15 K.

As shown in Figure 2, one proton on —NH_2 of $[tmgH]^+$ is transferred to —COO of $[L]^-$ by a TS where the hydrogen atom almost lies midway between N and O atoms. Finally, [tmgH][L] ion pair is transformed into tmg·HL molecular dimer, while ionic-type hydrogen bond is transformed into molecular-type hydrogen bond; where tmg is 1,1,3,3-tetramethylguanidine and HL is lactic acid. It can also be indicated that B3LYP/6-31++G** and MP2/6-31++G** give very similar structures.

The PES of proton transfer for [tmgH][L] is presented in Figure 3. Figure 3 shows that the energy barrier is very low for the proton transfer, and it is 1.5 kJ·mol^{-1} both at MP2/6-311++G(2df,p)//B3LYP/6-31++G** level and at MP2/6-311++G(2df,p)//MP2/6-31++G** level. The energy level of molecular collision is at ~20 kJ mol^{-1}, so the proton transfer energy barrier is almost negligible. When ZPE corrections are included, a much lower energy barrier is obtained (−8.0 kJ mol^{-1} at MP2/6-311++G(2df,p)//B3LYP/6-31++G** level and −11.2 kJ mol^{-1} at MP2/6-311++G(2df,p)//MP2/6-31++G** level). Such a negative energy barrier has been indicated for proton transfer reaction,[63,64] which is consistent with the nature of low energy barrier in proton transfer. The interesting finding is that the energy of tmg·HL molecular dimer is lower than that of [tmgH][L] ion pair. It is −2.3 kJ mol^{-1} (without ZPE correction) and −3.9 kJ mol^{-1} (with ZPE correction) lower at MP2/6-311++G(2df,p)//B3LYP/6-31++G** level; it is −2.0 kJ mol^{-1} (without ZPE correction) and −5.8 kJ mol^{-1} (with ZPE correction) at MP2/6-311++G(2df,p)//MP2/6-31++G** level. Thus, whether in terms of kinetics or thermodynamics, tmg·HL molecular dimer is a more favorable species than [tmgH][L] ion pair. This finding is also obtained for [tmgH][T] (Supporting Information Figure S1), where the transfer energy barrier is 2.0 kJ mol^{-1} (without ZPE correction) and −6.9 kJ mol^{-1} (with ZPE correction) at B3LYP/6-31++G** level, and the energy of tmg·HT molecule dimer is 0.9 kJ mol^{-1} lower than that of [tmgH][T] ion pair when ZPE correction is included.

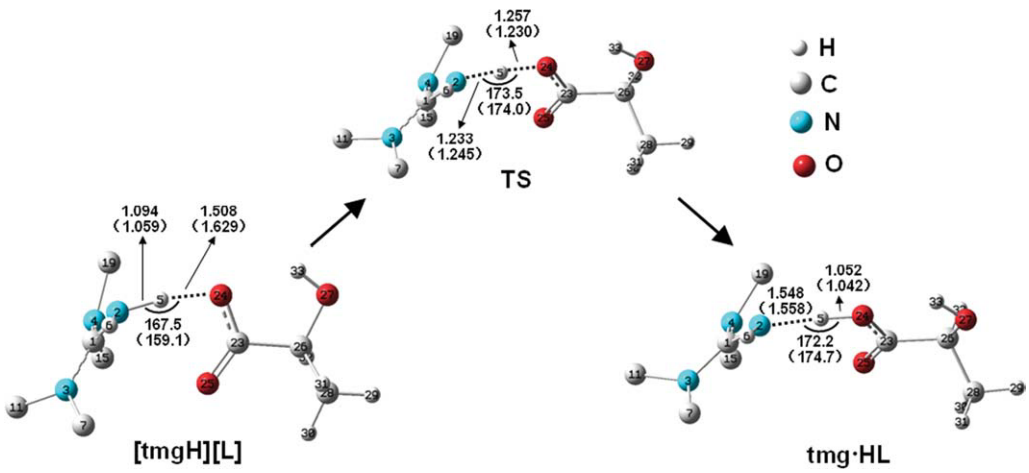

Figure 2. Reaction path for the proton transfer in [tmgH][L] ion pair (length in Å and angle in degree; the values in parentheses are at MP2/6-31++G level and the others are at B3LYP/6-31++G** level; some hydrogen atoms on $[tmgH]^+$ are screened for clarity).**

The color coding of atoms is used in all the figures. [Color figure can be viewed in the online issue, which is available at wileyonlinelibrary.com.]

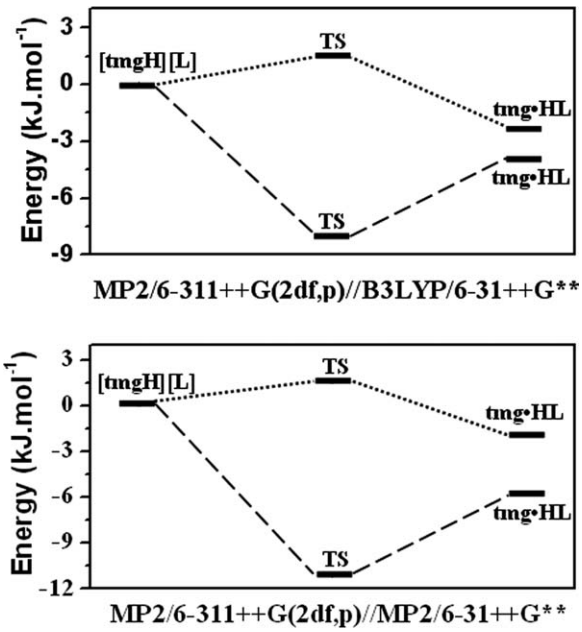

Figure 3. Reaction PES for the proton transfer in [tmgH][L] ion pair with ZPE corrections (dash lines) and without ZPE corrections (dot lines).

In addition, these calculation results show that the obtained structure and energy characteristic are similar at B3LYP/6-31++G** level and the higher levels. Therefore, for minimizing computational cost, the following calculations are performed only at B3LYP/6-31++G** level.

Trimer. Multi-ion cluster was found in the gas phase for some imidazolium-based ILs both from ab initio calculation[27,53] and mass spectrometric analysis.[37–40] Here, $[tmgH]^+$, $[L]^-$, tmg, and HL (including both ionic and molecular fragments), are added to tmg·HL dimer, respectively, to investigate the trimer. Similarly, $[tmgH]^+$, $[T]^-$, tmg, and HT, are added to tmg·HT dimer, respectively; $[tmgH]^+$, $[F]^-$, tmg, and HF are added to tmg·HF dimer, respectively. The most stable trimers that are finally obtained are presented in Figures 4a–d for [tmgH][L], in Supporting Information Figures S3a–d for [tmgH][T], and in Supporting Information Figures S4a–d for [tmgH][F]. As shown in Figures 4, Supporting Information S3, and S4, all the molecular dimers (tmg·HL, tmg·HT, tmg·HF) are retransformed into the ion pairs ([tmgH][L], [tmgH][T], [tmgH][F], respectively) with the addition of a third molecule or ion. Similar structure and energy characteristic are found for these three ILs. Therefore, only [tmgH][L] is selected to discuss the trimer in detail.

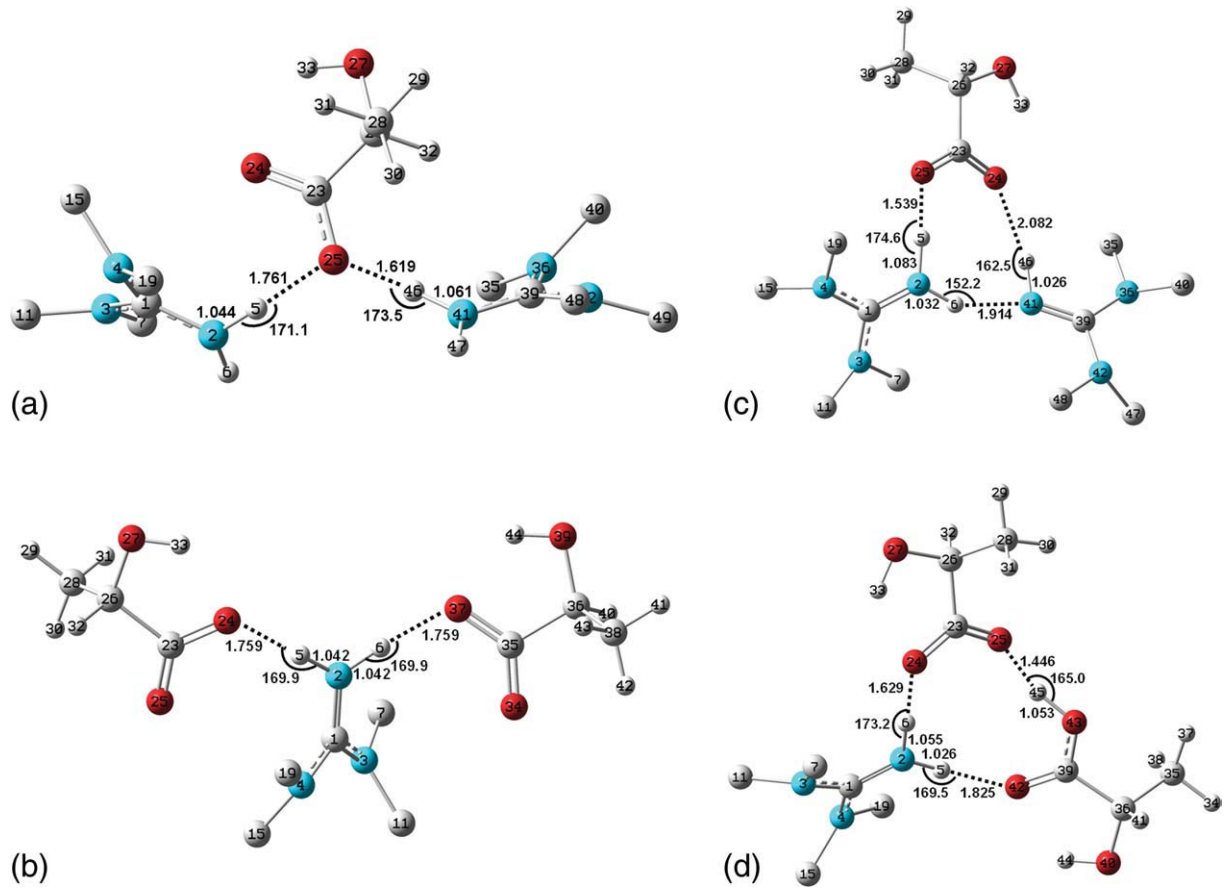

Figure 4. Trimer species in gas phase for [tmgH][L], obtained at B3LYP/6-31++G level (length in Å and angle in degree; some hydrogen atoms on $[tmgH]^+$ or tmg fragment are screened for clarity).**

(a) the addition of $[tmgH]^+$ to tmg·HL dimer; (b) the addition of $[L]^-$ to tmg·HL dimer; (c) the addition of tmg to tmg·HL dimer; (d): the addition of HL to tmg·HL dimer. [Color figure can be viewed in the online issue, which is available at wileyonlinelibrary.com.]

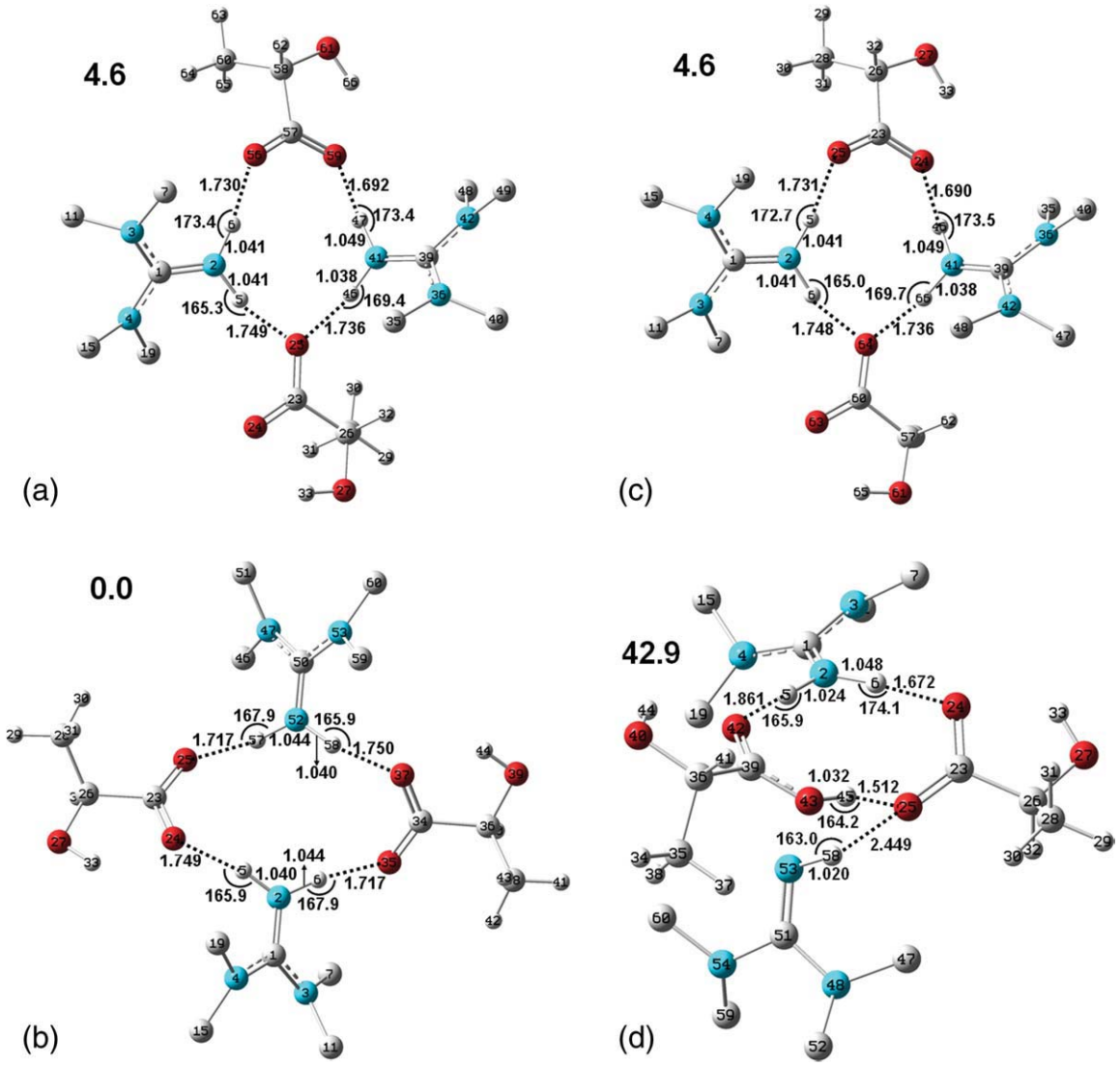

Figure 5. Tetramer species in gas phase for [tmgH][L], obtained at B3LYP/6-31++G level (length in Å and angle in degree; some hydrogen atoms on $[tmgH]^+$ or tmg fragment are screened for clarity; the relative energy values are also labeled in top-left corner). (a) the addition of [L]- to the trimer in Figure 4a; (b) the addition of $[tmgH]^+$ to the trimer in Figure 4b; (c) the addition of HL to the trimer in Figure 4c; (d) the addition of tmg to the trimer in Figure 4d.**

[Color figure can be viewed in the online issue, which is available at wileyonlinelibrary.com.]

From Figure 4, it is easily understood that the return of proton from HL to tmg can be ascribed to the strengthened proton-acceptability of N atom on $-NH_2$ and the weakened proton-acceptability of O atom on —COO, with the assistance of a third ionic or molecular fragment. Specifically, in Figure 4a, the hydrogen bond interaction between O atom on —COO and H atom on $-NH_2$ of added $[tmgH]^+$ weakens the proton-acceptability of O atom for the original proton. Finally, the hydrogen bond interaction is shared by two $[tmgH]^+$. Similarly, in Figure 4b, the hydrogen bond interaction between H atom on $-NH_2$ and O atom on —COO of added $[L]^-$ strengthens the proton-acceptability of N atom on $-NH_2$. In Figure 4c, the hydrogen bond interaction between H atom on $-NH_2$ and N atom on $-NH_2$ of added tmg strengthens the proton-acceptability of N atom on $-NH_2$, while the hydrogen bond interaction between O atom on —COO and H atom on $-NH_2$ of added tmg weakens the proton-acceptability of O atom. In Figure 4d, the hydrogen bond interaction between H atom on $-NH_2$ and O atom on —COO of added HL strengthens the proton-acceptability of N atom on $-NH_2$, while the hydrogen bond interaction between O atom on —COO and H atom on —OH of added HL weakens the proton-acceptability of O atom. In other words, addition of $[tmgH]^+$, [L]-, tmg, or HL will lead to reduction of tmg·HL dimer to[tmgH][L] ion pair.

Tetramer. The initial structures of the tetramers for [tmgH][L] are constructed by adding $[L]^-$, $[tmgH]^+$, HL, and tmg, to the trimers, as shown in Figures 4a–d

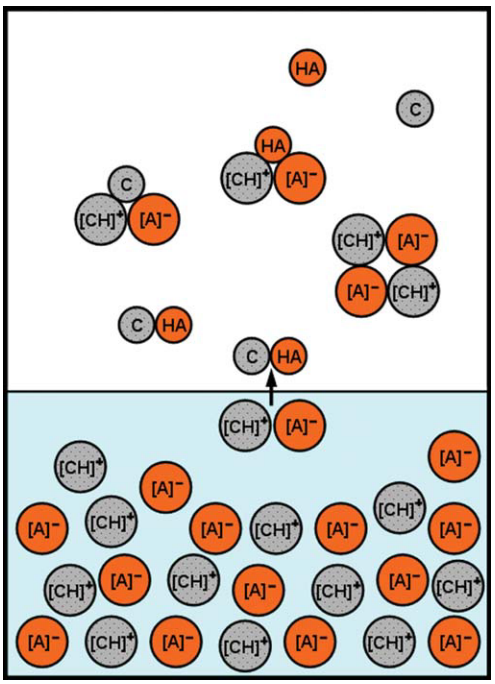

Figure 6. Schematic representation of volatilization of [tmgH][L], [tmgH][T], and [tmgH][F].

The above is gas phase and the below is liquid phase. $[CH]^+$, [A]-, C, and HA, represent cation 1,1,3,3-tetramethylguanidinium, anion (lactate, trifluoroacetate, or formate), 1,1,3,3-tetramethylguanidine, and acid molecule (lactic acid, trifluoroacetic acid, or formic acid, respectively). [Color figure can be viewed in the online issue, which is available at wileyonlinelibrary.com.]

respectively, and the constructed tetramers are neutral with zero net charge. Similarly, the initial tetramers for [tmgH][T] are constructed by adding $[T]^-$, $[tmgH]^+$, HT, and tmg, to the trimers, as shown in Supporting Information Figures S3a–d, respectively. The initial tetramers for [tmgH][F] are constructed by adding $[F]^-$, $[tmgH]^+$, HF, and tmg, to the trimers, as shown in Supporting Information Figures S4a–d respectively. The obtained stable tetramers are presented in Figures 5a–d for [tmgH][L], in Supporting Information Figures S5a–d for [tmgH][T], and in Supporting Information Figures S6a–d for [tmgH][F]. Similar structure and energy characteristic are obtained for these three ILs. Therefore, only [tmgH][L] is used to discuss the tetramer in detail.

It is interestingly found that all the tetramers exist in ion-pattern, except the tetramer in Figure 5d. Moreover, the energy of the tetramer in Figure 5d is 38.3 kJ mol^{-1} higher than the tetramer in Figure 5a, 42.9 kJ mol^{-1} higher than the tetramer in Figure 5b, and 38.3 kJ mol^{-1} higher than the tetramer in Figure 5c. Thus, it can be expected that ionic cluster will be the most favorable pattern for tetramer in [tmgH][L] gas phase, which is also found in [tmgH][T] tetramer (Supporting Information Figure S5) and in [tmgH][F] tetramer (Supporting Information Figure S6).

Volatilization mechanism

The above ab initio results indicate that isolated ion pairs might not stably exist in the gas phase for [tmgH][L], [tmgH][T], and [tmgH][F]; however, a third molecule or ion can stabilize the ion pairs. Furthermore, ionic tetramers can also stably exist in the gas phase. All of them explain why [tmgH][L], [tmgH][T], and [tmgH][F] exist as ions in the liquid phase. Therefore, as shown in Figure 6, a volatilization picture can be visualized. Taking [tmgH][L] for example, in the liquid phase, [tmgH][L] exists in the pattern of $[tmH]^+$ and $[L]^-$. When an ion pair is volatilized into gas phase, tmg·HL molecular dimer is easily formed at liquid-gas interface or gas phase (where the interactions between other ions and the ion pair disappear) because of interionic proton transfer. When tmg·HL molecular dimer is in the gas phase, it can be dissociated into tmg and HL molecules, or form more complex trimer, tetramer or other aggregated species at some temperature and pressure.

The work of Maginn and his coworkers showed that ion pair is the most possible volatile species; while the ab initio calculations in this work indicate that proton transfer occurs in ion pair for such 1,1,3,3-tetramethylguanidinium-based ILs in the gas phase. Therefore, the enthalpy of vaporization obtained from our simulations with the assumption of ion pair may not correspond to what could be measured experimentally.

Conclusions

To promote the study on the volatility of ILs, [tmgH][L], [tmgH][T], and [tmgH][F] are selected to investigate the volatility of 1,1,3,3-tetramethylguanidinium-based ILs. Their vaporization enthalpies are calculated by using molecular dynamic simulations, and the gas phase species are determined by using ab initio calculations. Interionic coulombic electrostatic and Van der Waals interactions offer the greatest contribution to the vaporization enthalpy; while intraionic bond, angle, and dihedral interactions also give remarkable contribution. The statistical results for bond, angle, and dihedral distributions show that ion conformations in liquid phase are different from that in gas phase, which explains the intraionic contributions. Different from some imidazolium-based ILs, the ion pairs of such guanidinium-based ILs cannot stably exist and are easily transformed into molecular dimers in the gas phase. Furthermore, the dimers may be dissociated into isolated molecular patterns, or be formed into trimers or tetramers with the addition of a third or fourth molecular fragment. Finally, following the simulation results, a volatilization mechanism is discussed.

Acknowledgments

This work was financially supported by National Natural Science Foundation of China (20806002, 20976005, 20776140), Beijing Natural Science Foundation (2103051), National Basic Research Program of China (2009CB219901), and the Young Scholars Fund of Beijing University of Chemical Technology (QN0801). The Chemical Grid Project of Beijing University of Chemical Technology is also highly appreciated for generously providing the computer sources.

Literature Cited

1. Appleby D, Hussey CL, Seddon KR, Turp JE. Room-temperature ionic liquids as solvents for electronic absorption spectroscopy of halide complexes. *Nature*. 1986;323:614–616.
2. Hussey CL. Room temperature haloaluminate ionic liquids-novel solvents for transition metal solution chemistry. *Pure Appl Chem*. 1988;60:1763–1772.

3. Wilkes JS. A short history of ionic liquids-from molten salts to neoteric solvents. *Green Chemistry*. 2002;4:73–80.
4. Brennecke JF, Maginn EJ. Ionic liquids: innovative fluids for chemical processing. *AIChE J*. 2001;47:2384–2389.
5. Rogers RD, Seddon KR. Ionic liquids-Solvents of the future? *Science*. 2003;302:792–793.
6. RogersRD, Seddon KR, editors. *Ionic Liquids: Industrial Applications to Green Chemistry*. Washington DC: Oxford University Press, 2002.
7. Rogers RD, Seddon KR, editors. *Ionic Liquids as Green Solvents: Progress and Prospects*. Washington, DC: Oxford University Press, 2002.
8. Seiler M, Jork C, Kavarnou A, Arlt W, Hirsch R. Separation of azeotropic mixtures using hyperbranched polymers or ionic liquids. *AIChE J*. 2004;50:2439–2454.
9. Endres F. Ionic liquids: promising solvents for electrochemistry. *Zeitschrift für Physikalische Chemie*. 2004;218:255–283.
10. Alonso L, Arce A, Francisco M, Rodríguez O, Soto A. Gasoline desulfurization using extraction with $[C_8mim][BF_4]$ ionic liquid. *AIChE J*. 2007;53:3108–3115.
11. Earle MJ, Esperanca JMSS, Gilea1 MA, Lopes JNC, Rebelo LPN, Magee JW, Seddon KR, Widegren JA. The distillation and volatility of ionic liquids. *Nature*. 2006;439:831–834.
12. Wasserscheid P. Volatility times for ionic liquids. *Nature*. 2006; 439:797.
13. Paulechka YU, Zaitsau DH, Kabo GJ, Strechan AA. Vapor pressure and thermal stability of ionic liquid 1-butyl-3-methylimidazolium Bis(trifluoromethylsulfonyl)amide. *Thermochim Acta*. 2005;439:158–160.
14. Zaitsau DH, Kabo GJ, Strechan AA, Paulechka YU, Tschersich A, Verevkin SP, Heintz A. Experimental vapor pressures of 1-alkyl-3-methylimidazolium bis(trifluoromethylsulfonyl)imides and a correlation scheme for estimation of vaporization enthalpies of ionic liquids. *J Phys Chem A*. 2006;110:7303–7306.
15. Rebelo LPN, Lopes JNC, Esperancüa JMSS, Filipe E. On the critical temperature, normal boiling point, and vapor pressure of ionic liquids. *J Phys Chem B*. 2005;109:6040–6043.
16. Swiderski K, McLean A, Gordon CM, Vaughan DH. Estimates of internal energies of vaporisation of some room temperature ionic liquids. *Chem Commun*. 2004;2178–2179.
17. Santos LMNBF, Lopes CJN, Coutinho JAP, Esperanca JMSS, Gomes LR, Marrucho IM, Rebelo LPN. Ionic liquids: first direct determination of their cohesive energy. *J Am Chem Soc*. 2007; 129:284–285.
18. de Andrade J, Böes ES, Stassen H. A force field for liquid state simulations on room temperature molten salts: 1-ethyl-3-methylimidazolium tetrachloroaluminate. *J Phys Chem B*. 2002;106:3546–3548.
19. Liu ZP, Huang SP, Wang WC. A refined force field for molecular simulation of imidazolium-based ionic liquids. *J Phys Chem B*. 2004;108:12978–12989.
20. de Andrade J, Böes ES, Stassen H. Computational study of room temperature molten salts composed by 1-alkyl-3-methylimidazolium cations-Force-field proposal and validation. *J Phys Chem B*. 2002;106:13344–13351.
21. Morrow TI, Maginn EJ. Molecular dynamics study of the ionic liquid 1-*n*-butyl-3-methylimidazolium hexafluorophosphate. *J Phys Chem B*. 2002;106:12807–12813.
22. Micaelo NM, Baptista AM, Soares CM. Parametrization of 1-butyl-3-methylimidazolium hexafluorophosphate/nitrate ionic liquid for the GROMOS force field. *J Phys Chem B*. 2006;110:14444–14451.
23. Shah JK, Brennecke JF, Maginn EJ. Thermodynamic properties of the ionic liquid 1-n-butyl-3-methylimidazolium hexafluorophosphate from Monte Carlo simulations. *Green Chem*. 2002;4:112–118.
24. Cadena C, Maginn EJ. Molecular simulation study of some thermophysical and transport properties of triazolium-based ionic liquids. *J Phys Chem B*. 2006;110:18026–18039.
25. Cadena C, Zhao Q, Snurr RQ, Maginn EJ. Molecular modeling and experimental studies of the thermodynamic and transport properties of pyridinium-based ionic liquids. *J Phys Chem B*. 2006;110:2821–2832.
26. Kelkar MS, Maginn EJ. Calculating the enthalpy of vaporization for ionic liquid clusters. *J Phys Chem B*. 2007;111:9424–9427.
27. Dieter KM, Dymek CJ Jr, Heimer NE, Rovang JW, Wilkes JS. Ionic structure and interactions in 1-ethyl-3-methylimidazolium chloride-$AlCl_3$ molten salts. *J Am Chem Soc*. 1988;110:2722–2726.
28. Sitze MS, Schreiter ER, Patterson EV, Freeman RG. Ionic liquids based on $FeCl_3$ and $FeCl_2$. Raman scattering and ab initio calculations. *Inorg Chem*. 2001;40:2298–2304.
29. Meng Z, Dölle A, Carper WR. Gas phase model of an ionic liquid: semi-empirical and ab initio bonding and molecular structure. *J Mol Struct (THEOCHEM)*. 2002;585:119–128.
30. Turner EA, Pye CC, Singer RD. Use of ab initio calculations toward the rational design of room temperature ionic liquids. *J Phys Chem A*. 2003;107:2277–2288.
31. Paulechka YU, Kabo GJ, Blokhin AV, Vydrov OA, Magee JW, Frenkel M. Thermodynamic properties of 1-butyl-3-methylimidazolium hexafluorophosphate in the ideal gas state. *J Chem Eng Data*. 2003;48:457–462.
32. Talaty ER, Raja S, Storhaug VJ, Dölle A, Carper WR. Raman and infrared spectra and ab initio calculations of C2-4mim imidazolium hexafluorophosphate ionic liquids. *J Phys Chem B*. 2004;108:13177–13184.
33. Hunt PA, Kirchner B, Welton T. Characterising the electronic structure of ionic liquids: an examination of the 1-butyl-3-methylimidazolium chloride ion pair. *Chem Eur J*. 2006;12:6762–6775.
34. Hunt PA, Gould IR. Structural characterization of the 1-butyl-3-methylimidazolium chloride ion pair using ab initio methods. *J Phys Chem A*. 2006;110:2269–2282.
35. Schmidt MW, Gordon Ms, Boatz JA. Triazolium-based energetic ionic liquids. *J Phys Chem A*. 2005;109:7285–7295.
36. Alavi S, Thompson DL. Proton transfer in gas-phase ammonium dinitramide clusters. *J. Chem. Phys*. 2003, 18:25992605.
37. Bini R, Bortolini O, Chiappe C, Pieraccini D, Siciliano TJ. Development of cation/anion "interaction" scales for ionic liquids through ESI-MS measurements. *J Phys Chem B*. 2007;111:598–604.
38. Dupont J. On the solid, liquid and solution structural organization of imidazolium ionic liquids. *J Braz Chem Soc*. 2004;15:341–350.
39. AbdulSada AK, Elaiwi AE, Greenway AM, Seddon KR. Evidence for the clustering of substituted imidazolium salts via hydrogen bonding under the conditions of fast atom bombardment mass spectrometry. *Eur Mass Spect*. 1997;3:245–247.
40. Gozzo FC, Santos LS, Augusti R, Consorti CS, Dupont J, Eberlin MN. Gaseous supramolecules of imidazolium ionic liquids: "magic" numbers and intrinsic strengths of hydrogen bonds. *Chem Eur J*. 2004;10:6187–6193.
41. Xin X, Guo X, Duan H, Lin Y, Sun H. Efficient Knoevenagel condensation catalyzed by cyclic guanidinium lactate ionic liquid as medium. *Catal Commun*. 2007;8:115–117.
42. Fang S, Yang L, Wei C, Jiang C, Tachibana K, Kamijima K. Ionic liquids based on guanidinium cations and TFSI anion as potential electrolytes. *Electrochim Acta*. 2009;54:1752–1756.
43. Kulkarni PS, Branco LC, Crespo JG, Afonso CAM. A comparative study on absorption and selectivity of organic vapors by using ionic liquids based on imidazolium, quaternary ammonium, and guanidinium cations. *Chem Eur J*. 2007;13:8470–8477.
44. Mateus NMM, Branco LC, Lourenço NMT, Afonso CAM. Synthesis and properties of tetra-alkyl-dimethylguanidinium salts as a potential new generation of ionic liquids. *Green Chem*. 2003;5:347–352.
45. Xie H, Zhang S, Duan H. An ionic liquid based on a cyclic guanidinium cation is an efficient medium for the selective oxidation of benzyl alcohols. *Tetrahedron Lett*. 2004;45:2013–2015.
46. Gao H, Han B, Li J, Jiang T, Liu Z, Wu W, Chang Y. Preparation of room-temperature ionic liquids by neutralization of 1,1,3,3-tetramethylguanidine with acids and their use as media for mannich reaction. *Synth Commun*. 2004;34:3083–3089.
47. Zhang SJ, Yuan XL, Chen YH, Zhang XP. Solubilities of CO_2 in 1-butyl-3-methylimidazolium hexafluorophosphate and 1,1,3,3-tetramethylguanidium lactate at elevated pressures. *J Chem Eng Data*. 2005;50:1582–1585.
48. Yu G, Zhang S, Liu X, Zhou G, Chen X. Structure, interaction and property of amino-functionalized imidazolium ionic liquids by ab initio calculation and molecular dynamics simulation. *AIChE J*. 2007;53:3210–3221.
49. Yu G, Zhang S, Yao X, Zhang J, Dong K, Dai W, Mori R. Design of task-specific ionic liquids for capturing CO_2: a molecular orbital study. *Ind Eng Chem Res*. 2006;45:2875–2880.
50. Yu G, Zhang S. Insight into the cation-anion interaction in 1,1,3,3-tetramethylguanidinium lactate ionic liquid. *Fluid Phase Equilibria*. 2007;255:86–92.

51. Liu X, Zhang S, Zhou G, Wu G, Yuan X, Yao X. New force field for molecular simulation of guanidinium-based ionic liquids. *J Phys Chem B*. 2006;110:12062–12071.
52. Zhou G, Liu X, Zhang S, Yu G, He H. A force field for molecular simulation of tetrabutylphosphonium amino acid ionic liquids. *J Phys Chem B*. 2007;111:7078–7084.
53. Dong K, Zhang S, Wang D, Yao X. Hydrogen bonds in imidazolium ionic liquids. *J Phys Chem A*. 2006;110:9775–9782.
54. Liu X, Zhou G, Zhang S. Molecular dynamics simulation of acyclic guanidinium-based ionic liquids. *Fluid Phase Equilibria*. 2008; 272:1–7.
55. Lyubartsev AP, Laaksonen AM. DynaMix–a scalable portable parallel MD simulation package for arbitrary molecular mixtures. *Comput Phys Commun*. 2000;128:565–589.
56. Frisch MJ, Trucks GW, Schlegel HB, Scuseria GE, Robb MA, Cheeseman JR, Montgomery JA Jr, Vreven T, Kudin KN, Burant JC, Millam JM, Iyengar SS, Tomasi J, Barone V, Mennucci B, Cossi M, Scalmani G, Rega N, Petersson GA, Nakatsuji H, Hada M, Ehara M, Toyota K, Fukuda R, Hasegawa J, Ishida M, Nakajima T, Honda Y, Kitao O, Nakai H, Klene M, Li X, Knox JE, Hratchian HP, Cross JB, Adamo C, Jaramillo J, Gomperts R, Stratmann RE, Yazyev O, Austin AJ, Cammi R, Pomelli C, Ochterski JW, Ayala PY, Morokuma K, Voth GA, Salvador P, Dannenberg JJ, Zakrzewski VG, Dapprich S, Daniels AD, Strain MC, Farkas O, Malick DK, Rabuck AD, Raghavachari K, Foresman JB, Ortiz JV, Cui Q, Baboul AG, Clifford S, Cioslowski J, Stefanov BB, Liu G, Liashenko A, Piskorz P, Komaromi I, Martin RL, Fox DJ, Keith T, Al-Laham MA, Peng CY, Nanayakkara A, Challacombe M, Gill PMW, Johnson B, Chen W, Wong MW, Gonzalez C, Pople JA. *GAUSSIAN 03 Revision C. 02*. Wallingford CT: Gaussian, Inc., 2004.
57. Møller C, Plesset MS. Note on an approximation treatment for many-electron systems. *Phys Rev*. 1934;46:618–622.
58. Pople JA, Binkley JS, Seeger R. Theoretical models incorporating electron correlation. *Int J Quantum Chem Symp*. 1976;10:1–19.
59. Becke AD. Density-functional thermochemistry. III. The role of exact exchange. *J Chem Phys*. 1993;98:5648–5652.
60. Lee C, Yang W, Parr RG. Development of the Colle-Salvetti correlation-energy formula into a functional of the electron density. *Phys Rev B*. 1988;37:785–789.
61. Dzyuba SV, Bartsch RA. Influence of structural variations in 1-alkyl(aralkyl)-3-methylimidazolium hexafluorophosphates and bis(trifluoromethylsulfonyl)imides on physical properties of the ionic liquids. *ChemPhysChem*. 2002;3:161–166.
62. LideDR, editor. *Handbook of Chemistry and Physics*, 80th ed. Boca Raton, FL: CRC Press, 1999-2000.
63. Koch W, Holthausen MC. *A Chemist's Guide to Density Functional Theory*, 2nd ed. Weinheim, Germany: Wiley-VCH Verlag GmbH, 2001.
64. Goumri A, Rocha JDR, Laakso D, Smith CE, Marshall P. Characterization of reaction pathways on the potential energy surfaces for H + SO_2 and HS + O_2. *J Phys Chem A*. 1999;103:11328–11335.

Manuscript received Jun. 29, 2009, and revision received Mar. 19, 2010.